Magnetic Resonance in Medicine 45:349–355 (2001)

Study of Tricarboxylic Acid Cycle Flux Changes in Human Visual Cortex During Hemifield Visual Stimulation Using ^{1}H-{^{13}C} MRS and fMRI

Wei Chen,* Xiao-Hong Zhu, Rolf Gruetter, Elizabeth R. Seaquist, Gregor Adriany, and Kamil Ugurbil

The relationships between brain activity and accompanying hemodynamic and metabolic alterations, particularly between the cerebral metabolic rate of oxygen utilization (CMR_{O2}) and cerebral blood flow (CBF), are not thoroughly established. CMR_{O2} is closely coupled to the rate of tricarboxylic acid (TCA) cycle flux. In this study, the changes in glutamate labeling during ^{13}C labeled glucose administration were determined in the human brain as an index of alterations in neuronal TCA cycle turnover during increased neuronal activity. Two-volume ^{1}H-{^{13}C} MR spectroscopy (MRS) of the visual cortex was combined with functional MRI (fMRI) at 4 Tesla. Hemifield visual stimulation was employed to obtain data simultaneously from activated and control regions located symmetrically in the two hemispheres of the brain. The results showed that the fractional change in the turnover rate of C4 carbon of glutamate was less than that of CBF during visual stimulation. The fractional changes in CMR_{O2} (ΔCMR_{O2}) induced by activation must be equal to or less than the fractional change in glutamate labeling kinetics. Therefore, the results impose an upper limit of ~30% for ΔCMR_{O2} and demonstrate: 1) that fractional CBF increases exceed ΔCMR_{O2} during elevated activity in the visual cortex, and 2) that such an unequal change would explain the observed positive blood oxygenation level dependent (BOLD) effect in fMRI. Magn Reson Med 45:349–355, 2001.

Key words: cerebral oxygen utilization; tricarboxylic acid cycle flux; human visual cortex; hemifield visual stimulation; ^{1}H-{^{13}C} MRS; functional MRI; neuronal activity

Minimally invasive or noninvasive imaging techniques, such as positron-emission tomography (PET), optical imaging, and BOLD-based fMRI (1–3) are employed with increasing frequency in studies of brain function. These methods, however, do not measure electrical activity of the brain directly; instead, they rely on secondary metabolic and hemodynamic responses. The preeminence of these imaging techniques in contemporary neuroscience research has highlighted the fact that many aspects of these metabolic and hemodynamic responses remain poorly understood and controversial. The central question in this controversy is the effect of elevated neuronal activity on regional cerebral metabolism of oxygen utilization rate (CMR_{O2}).

Under resting conditions, total glucose consumption rate in the brain (CMR_{glc}) is well coupled to CMR_{O2} and to cerebral blood flow (CBF) in the human brain (4), and occurs predominantly through oxidation. However, it has been suggested that this may not be the case during increased neuronal activity. Based on PET measurements, the increases of CMR_{O2} (0–5%) were reported to be much less than the elevation in CBF and CMR_{glc} (40–51%) during visual and somatosensory stimulation, suggesting that CMR_{O2} is "uncoupled" from CBF and CMR_{glc} in the activated state (5,6). This concept, however, is counterintuitive in view of the large aerobic capacity in the brain. The difficulties associated with PET, which relies on multiple independent measurements and intersubject averaging to determine CMR_{O2}, have also contributed to the skepticism about the validity of this concept. Because of this complexity, only a few such PET measurements have been reported, with discrepant conclusions.

Resolution of this problem requires new studies on CMR_{O2}, especially using techniques that are dependent on entirely new mechanisms. Measurements in a single subject within a single experiment are also crucial in order to avoid large variances generated by intersubject averaging. Cerebral oxygen consumption is coupled to tricarboxylic acid (TCA) cycle flux, which can be assessed using MR spectroscopy and ^{13}C-labeled substrate infusion. The technique relies on measuring the isotopic turnover rate of glutamate (Glu) from infused [1-^{13}C] labeled glucose using direct detection of ^{13}C or indirect detection through coupled protons (^{1}H-{^{13}C} MRS technique) (7–9). These approaches have been used for basal measurements of TCA cycle turnover rate in the human brain (8,9) and changes associated with forepaw electrical stimulation in animal studies (10).

The availability of high magnetic fields provides the possibility for the first time that similar spectroscopic techniques (7) can be employed simultaneously with imaging to determine metabolic consequences of elevated neural activity in the awake human brain in single subjects. In this work, we report the results of such a study conducted at 4 Tesla using a two-volume ^{1}H-{^{13}C} MRS technique combined with fMRI and hemifield visual stimulation that selectively activates the primary visual cortex

Center for Magnetic Resonance Research, Radiology Department, University of Minnesota School of Medicine, Minneapolis, Minnesota.

Grant sponsor: NIH; Grant numbers: RR08079 (NCRR); NS38070; NS35192; NS38672; NS39043; Grant sponsor: Whitaker Foundation; Grant sponsor: NCRR; Grant numbers: P41 RR08079; M01RR00400.

*Correspondence to: Wei Chen, Ph.D., Center for Magnetic Resonance Research, Radiology Department, University of Minnesota School of Medicine, 2021 Sixth Street S.E., Minneapolis, MN 55455. E-mail: wei@cmrr.umn.edu

Received 25 July 2000; revised 26 October 2000; accepted 7 November 2000.

(V1) area in the contralateral hemisphere. The data were analyzed using a model accounting for glial and neuronal compartments to determine the impact of activation on the rate of neuronal pyruvate dehydrogenase, V_{PDH}, as a measure of neuronal TCA cycle activity, and therefore oxygen utilization rate in the brain.

MATERIALS AND METHODS

Visual Stimulus

The hemifield visual stimulus with reversal checkerboard pattern (full visual field = 44° width × 34° height) was presented on a screen inside a magnet which could be viewed by subjects via a mirror. The checkerboard was reversed at an 8-Hz frequency between red and black colors. The side of the hemifield visual stimulation was randomly chosen for different subjects. A small cross-shaped marker at the center served as a central fixation point, and the orientation of this marker was rotated by 45° at random intervals. Subjects were asked to maintain fixation on the marker during both control and task periods, and to respond to the rotation of the marker by pressing a button. The responses were evaluated, and the correct response rates were above 90%.

Human Studies

Five healthy subjects (two males and three females, 26–31 years of age, average 29 years) without history of neurological disorders participated in this study, which was approved by the institutional review board of the University of Minnesota. Prior to the experiment, subjects were prepared for the study with the placement of intravenous catheters in each arm. Somatostatin was infused at a rate of 0.16 μg/kg/min through one catheter, and glucose was infused through the other. A third catheter was placed in the distal leg for the collection of blood samples every 5 min. When baseline sampling was complete and hemifield visual stimulation and MRS acquisition were started, subjects were given a bolus injection of 30 g of 99% enriched [1-^{13}C] D-glucose (20% weight/volume), according to recently-described procedures (9). Plasma glucose was then maintained at the peak level by the infusion of 70% enriched [1-^{13}C] D-glucose (20% weight/volume) at a variable rate. After 20 g of additional [1-^{13}C] D-glucose had been infused (or approximately 20 min after the bolus injection), all glucose infusions were stopped and plasma glucose was allowed to decrease to baseline. ^{1}H-{^{13}C} MRS data were obtained during the entire infusion period (74–90 min for four subjects and 48 min for subject 3) with hemifield visual stimulation.

NMR Experiments

All studies were conducted on a Varian (Palo Alto, CA) console interfaced to a Siemens (Erlangen, Germany) 4 Tesla whole body MRI/MRS system. The same surface-coil probe was used for both fMRI and MRS measurements, consisting of a 10-cm single loop surface coil with distributed capacitance for ^{1}H excitation and reception and two 15-cm surface coils in quadrature mode for ^{13}C spin inversion and decoupling. A 1-cm diameter sphere containing [^{13}C]-formic acid was placed at the center of the ^{1}H coil for calibrating the ^{13}C-radiofrequency power. Multislice (128 × 128 matrix size) T_1-weighted turbo fast low-angle shot (turboFLASH) images were acquired for anatomical information.

Functional MRI Acquisition

An fMRI study was performed on each subject using the hemifield visual stimulation prior to the ^{13}C measurements. The purpose of these initial fMRI examinations was: 1) to ensure that the hemifield visual stimulation only activated the V1 area in the contralateral hemisphere; and 2) to determine the location and size of the activated area, based on which the localized volume for spectroscopy was specified. Seven contiguous coronal slices covering the calcarine fissure were acquired using a gradient echo-planar imaging (EPI) sequence (64 × 64 image matrix size, 20 × 20-cm^2 field of view, 5-mm slice thickness, TE = 25–38 msec, TR = 2 sec). Three control periods and two task periods were designed in an interleaved way; 20 image sets were acquired in each of the five consecutive periods, resulting in a total of 100 multislice image sets.

Prior to 2D Fourier transformation, the *k*-space imaging data was apodized with Gaussian filtering to improve the signal-to-noise ratio (SNR), resulting in a ~0.3 pixel increase in pixel size at full width at half maximum (FWHM) (11). Time courses were analyzed using functional imaging software STIMULATE, developed in our laboratory. Activation maps were generated by statistical parametric mapping using the period cross-correlation statistic method (12). "Activated" pixels were determined by requiring that the cross-correlation coefficient (cc) was 0.3 or higher, and a four-pixel neighborhood cluster was present. Using a method (11) that accounts for the 1) cluster size threshold (= 4); 2) threshold of statistical significance (t or z value = 3.05); 3) smoothness due to the Gaussian filtering; and 4) total number of pixels in the searched brain area (~1000 for a single slice), the effective *P* value was calculated to be 0.017. The fMRI maps were used for guiding the voxel position of the localized ^{1}H-{^{13}C} MRS and for calculating the fractional activation volume (F_{AV}) within the voxel. The values of F_{AV} were used for partial volume correction for calculating the relative changes of CMR_{O2} during visual stimulation. Potential differences in gray matter content in the voxels was assumed to be negligible, given the symmetric placement of the volume of interest (VOI) relative to the central sulcus and the symmetry of normal brain.

^{1}H-{^{13}C} MRS Measurements

The measurements of glutamate labeling kinetics were based on the ^{1}H-{^{13}C} MRS technique (7,8), implemented as described previously (7). Briefly, the pulse sequence consisted of: 1) spatial localization using point-resolved spectroscopy (PRESS) (13), 2) outer volume suppression combined with water suppression, 3) a ^{13}C inversion pulse (0.56 msec) centered at $1/(2J_{CH})$ ~ 4 msec for heteronuclear editing, and 4) Wideband Alternating-phase Low-power Technique for Zero-residual splitting decoupling (WALTZ)-16 pulses for broadband ^{13}C decoupling. The

average specific absorption rate (SAR) for the entire pulse sequence was below the FDA guideline. Subtractions of the two free induction decays (FIDs) acquired in the presence and absence of the ^{13}C inversion pulse yielded edited spectra containing only signals from protons coupled to ^{13}C nuclei (8). Additions of these paired FIDs resulted in ^{1}H spectra containing signals from protons attached to ^{12}C spins only. In this study, the pulse sequence (7) was further modified based on the concept of multivolume localization for simultaneous detection of two ^{1}H-{^{13}C} spectra from two adjacent localized volumes in a single experiment. This was accomplished by adding an adiabatic inversion pulse that was only used during alternate block acquisitions of ^{1}H-{^{13}C} spectra; this adiabatic pulse inverted half of the original localized volume along the direction perpendicular to the central fissure. Addition and subtraction of these two interleaved block data provided two ^{1}H-{^{13}C} spectra (mainly containing the ^{1}H resonance peaks of Glu C4) from the two adjacent V1 areas located in the left and right hemispheres, respectively ($1.5 \times 2.0 \times 2.0 = 6$ cm^3 each side). Spectral parameters were: TE = 23 msec, TR = 3 sec, 2048 complex data points, 4000 Hz spectral width, and 64 scans for each pair of ^{1}H-{^{13}C} spectra from the left- and right-hemisphere V1 areas. Prior to fast Fourier transformation, the FID was zero-filled and multiplied with an exponential function corresponding to a 1-Hz line broadening. The edited ^{1}H-{^{13}C} spectra were used for integrating the proton resonance peaks from Glu $^{13}C4$ (2.20–2.45 ppm), Glu $^{12}C4$ (2.20–2.45 ppm), and ^{12}C *total* creatine (i.e., tCr) (2.9–3.1 ppm), respectively. A linear baseline correction was applied prior to the integration.

The averaged ^{1}H-{^{13}C} spectra from the last 8–12 spectra were used to calculate fractional enrichment (FE) of ^{13}C labeled Glu C4 based on the equation of FE = [Glu $^{13}C4$]/([Glu $^{13}C4$] + [Glu $^{12}C4$]) for both activated and control voxels. Generally, the NMR sensitivities of detection by the surface coil between the left- and right-hemisphere V1 regions were not identical, as expected. To determine whether the steady-state concentrations of Glu $^{12}C4$ and Glu $^{13}C4$ were the same on both sides, we compared the relative signal of tCr (i.e., $tCr_{(left\ voxel)}$/ $tCr_{(right\ voxel)}$) to the analogous ratios calculated for the Glu $^{12}C4$ and Glu $^{13}C4$ resonances. Linear regression yielded a unit slope for both comparisons (slope = 0.95, correlation coefficient γ = 0.99, and P = 0.01 for the [tCr] ratio vs. [Glu $^{12}C4$] ratio; and slope = 1.06, correlation coefficient γ = 0.98, and P = 0.02 for the [tCr] ratio vs. [Glu $^{13}C4$] ratio). Assuming that total creatine content does not change during visual stimulation and is the same at both locations, we concluded that [Glu $^{13}C4$] and [Glu $^{12}C4$] at steady states were similar between the activated and control voxels. Therefore, the steady state of Glu $^{13}C4$ signal intensities were used to normalize the Glu $^{13}C4$ intensities at all time points, and these normalized curves were then used.

Calculation of Fractional Change in Neuronal Pyruvate Dehydrogenase Rate (V_{PDH})

The normalized glutamate [4-^{13}C] labeling data were analyzed for fractional changes in the rate of neuronal pyruvate dehydrogenase (V_{PDH}). This was accomplished using a two-compartment model (Ref. 9 and references therein) that accounts for glial/neuronal compartmentation of the TCA cycle with large (neuronal) and small (glial) glutamate pools. Neuronal V_{PDH} dominates carbon substrate entry into the neuronal TCA cycle in the virtual absence of anaplerosis in the neuronal compartment (Ref. 9 and references therein), especially when only the C4 carbon of glutamate is monitored, as was done in this study. Therefore, fractional changes in V_{PDH} reflect fractional changes of neuronal TCA cycle rate in tissue. The analysis for determining this fractional change was performed with or without modeling possible effects of increased glucose consumption rate on the ^{13}C fractional enrichment kinetics of the cerebral glucose pool.

Label turnover of brain glucose was either assumed to be independent of the glucose consumption rate or the effect of brain glucose turnover (14) was evaluated from the kinetic constants of the reversible Michaelis-Menten model of glucose transport (15). The latter was achieved similarly to previous studies (9,16) by solving the corresponding differential equations for changes in total brain glucose and 1-^{13}C brain glucose to generate a curve describing the change in fractional enrichment of pyruvate, assuming a 1 μmol/g brain lactate concentration (17). A potential 50% increase in brain lactate was assumed to have a negligible impact on the labeling of acetyl-CoA, given the high activity of lactate dehydrogenase (LDH) and the high surface area of the brain cell membranes.

The following assumptions were used in the two-compartment model for the determination of V_{PDH}: The exchange rate between mitochondrial α-ketoglutarate and cytosolic glutamate, V_x, was assumed to be 57 μmol/g and [Glu] = 9.0 μmol/g. The assumption that α-ketoglutarate and glutamate exchange is very fast was based on previous reports in brain (16,18). This assumption may not be true in all tissues and under all conditions, as was shown in the heart. Therefore, we also evaluated the case in which the exchange rate V_x was equal to the flux through the neuronal TCA cycle. The flux through (glial) glutamine synthetase V_{syn} was set to ~0.25 μmol/g/min, which is the rate of glutamine synthesis reported with a one-compartment model (referred to as V_{Gln} in that model) (16), and the rate of the glial enzyme pyruvate carboxylase, V_{pc}, was set to 20% V_{syn} (9,19). For fitting, Glu was normalized and expressed as a percentage of the steady-state signal.

The following two metabolic rates were adjusted to provide the best fit to the experimental data: 1) the rate of label dilution by efflux of lactate and pyruvate, V_{out}, and 2) (neuronal) $V_{PDH.}$ V_{out} accounts for a decreased fractional enrichment in Glu relative to half that of plasma glucose (10).

Partial Volume Correction of V_{PDH} Calculation

The partial volume correction for V_{PDH} observed by fMRS is given by

$$V_{PDH,Observed} = F_{AV} \cdot V_{PDH,Activated} + (1 - F_{AV}) V_{PDH,Control} \quad [1]$$

where $V_{PDH,Observed}$, $V_{PDH,Activated}$, and $V_{PDH,Control}$ are the V_{PDH} rates detected during the visual stimulation before

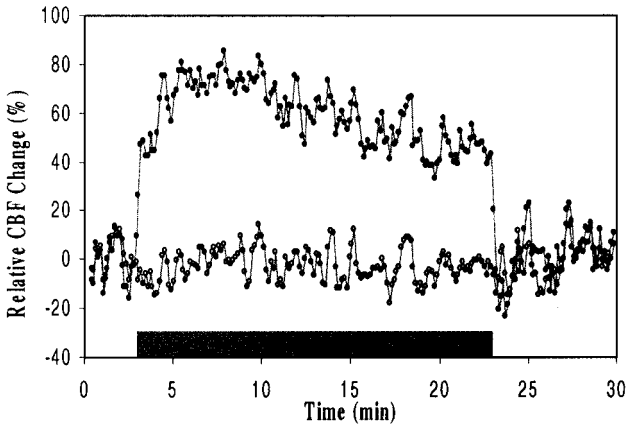

FIG. 1. Time courses of CBF change from the activated V1 (solid circles) and control V1 (open circle). The dark bar indicates the task period of visual stimulation.

and after the partial volume correction and during resting condition, respectively. Based on the definitions of

$$\left(\frac{\Delta V_{PDH}}{V_{PDH}}\right)_{\text{Observed or Corrected}} = \frac{V_{PDH,\text{ Observed or Activated}} - V_{PDH,\text{ Control}}}{V_{PDH^{\text{Control}}}} \quad [2]$$

one can get a simple relationship between corrected and observed values of $\Delta V_{PDH}/V_{PDH}$ using Eq. [1]

$$\left(\frac{\Delta V_{PDH}}{V_{PDH}}\right)_{Corrected} = \frac{1}{F_{AV}}\left(\frac{\Delta V_{PDH}}{V_{PDH}}\right)_{Observed}. \quad [3]$$

All data are presented as mean ± SEM.

RESULTS

Sustained Response During Prolonged Stimulation

Most fMRI studies use relatively short task periods (0.5–1 min). However, MRS experiments for investigating metabolic changes during functional activity (10), and the present experiments require relatively long data acquisition periods (on the order of 40–60 minutes) and, ultimately, long stimulation duration. Interpretation of these long functional experiments requires an understanding of the metabolic and neuronal activity changes during sustained stimulation. We previously reported that the BOLD effect remained detectable during sustained visual stimulation (up to 15 min) in the human brain (20). Prior to the spectroscopy studies reported in this work, we used the flow-sensitive alternating inversion recovery (FAIR) perfusion technique (21) to reexamine whether CBF remains increased during a sustained hemifield visual stimulation (20–30 min). Figure 1 illustrates CBF data from an individual subject. The results indicated that a significant CBF increase in the activated V1 areas (contralateral hemisphere) persists during the entire stimulation period (20 min). No significant increase of CBF was observed in the control V1 areas. Therefore, it is feasible to utilize MRS for studying metabolic response during a sustained visual stimulation in the human brain.

Functional MRI and ^{1}H-{^{13}C} MRS

In each subject, selective V1 activation of the contralateral hemisphere by hemifield stimulation was experimentally verified by fMRI. Figure 2 illustrates multislice fMRI maps (two contiguous coronal slices) from a single subject during left hemifield stimulation, showing activation only in the contralateral (right) hemisphere (Fig. 2a). The in-plane activation size was approximately 2 × 1.5 cm^2 and was similar to the size used for ^{1}H-{^{13}C} MRS studies (the dark-line box in Fig. 2a). Figure 2b displays the BOLD time courses from the activated V1 (top line, ~5% BOLD increase) and control V1 (lower line) from the same subject. There was no significant BOLD response in the control V1 area (the white-line box in Fig. 2a). These fMRI maps were also used to calculate F_{AV} (see Methods section) in the activated V1 for each subject, as listed in Table 1. The conservative choice of the statistical significance for the activation threshold employed in these studies implies that the reported F_{AV} is a *lower limit* of the activated volume measured by BOLD fMRI. Nevertheless, the averaged F_{AV} was high (0.81 ± 0.09, $N = 5$).

Figure 3 displays the plots of serial ^{1}H-{^{13}C} spectra (64 scans, 3-min acquisition time and 6-cm^3 localized volume) of [4-^{13}C] Glu obtained from the activated (Fig. 3a) and control (Fig. 3b) V1 areas, respectively, during hemifield visual stimulation and concomitant [1-^{13}C] glucose infusion from a single subject. [4-^{13}C] Glu isotopic labels from both the activated and control V1 areas increased as a function of infusion time at a similar rate, suggesting that small (if any) differences in metabolism were present between the hemispheres. The steady-state FE of [4-^{13}C] Glu

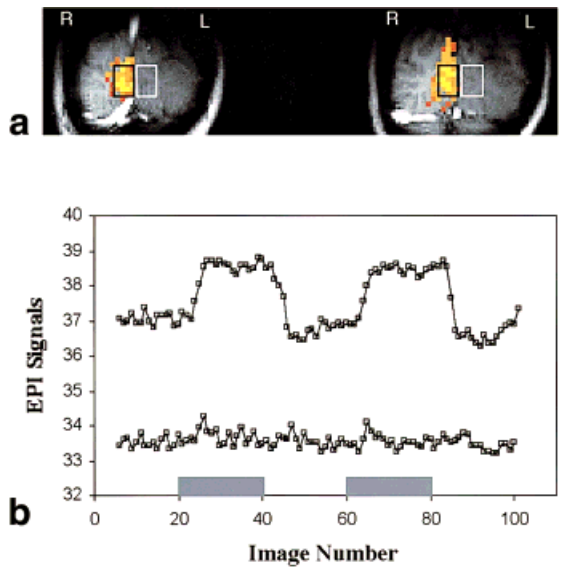

FIG. 2. **a:** Functional MR images (two contiguous coronal slices) from a single subject during the left hemifield visual stimulation. The stimulation activated the V1 areas in the contralateral (right) hemisphere alone. **b:** BOLD time courses from the activated V1 (top line, ~5% BOLD increase, the dark-line box) and control V1 (lower line, the white-line box). The boxes indicate the voxel volumes (2 × 1.5 cm^2) and positions used for ^{1}H-{^{13}C} MRS studies. The symbols L and R represent the left and right hemispheres, respectively. The dark bars indicate the task periods of visual stimulation.

Table 1
Summary of Glutamate Turnover Rate Changes in the Human Brain During Visual Stimulation

Subject	Activated hemisphere	Fractional enrichment (%)		F_{av}	Increase of [4-^{13}C] Glu turnover rate (%)
		Activated	Control		
1	Left	19.3	18.2	0.88	0.20
2	Right	17.1	18.3	1.00	0.28
3	Right	16.5	14.0	0.90	0.75
4	Left	19.0	17.5	0.70	0.14
5	Left	19.2	17.8	0.50	0.01
Mean		18.2	17.2	0.81	0.28
SEM		0.6	0.8	0.09	0.12

was not statistically different ($P = 0.16$ for paired t-test) between the activated V1 (18.2 ± 0.6; $N = 5$) and control V1 (17.2 ± 0.8; $N = 5$) (see Table 1).

Calculation of V_{PDH} Changes

The time courses of [4-^{13}C] Glu isotopic labeling from the activated and control V1 areas and the best fits of the metabolic modeling to the data from the same subject (Fig. 3) are shown in Fig. 4a. Figure 4b illustrates the analogous time courses and the best fits obtained after averaging the results from all subjects ($N = 5$). A slightly faster rate of [4-^{13}C] Glu isotopic labeling was observed on the activated side for all individuals, as well as for the intersubject averaged data.

Metabolic modeling (see Methods section) indicated that V_{PDH} was 0.83 ± 0.13 μmol/g/min under basal conditions, consistent with measurements of glucose consumption rate (CMR_{glc} = 0.42 μmol/g/min in the human visual cortex (6)), and increased to 1.12 ± 0.20 μmol/g/min (mean ± SEM) during visual stimulation. When calculated in this way, V_{PDH} did not statistically differ between activated and nonactivated voxels because of the large interindividual scatter. However, because of the paired nature of our study design, a more reliable comparison based on the *fractional* changes in V_{PDH} was performed. This analysis showed that V_{PDH} in the activated volume *relative* to

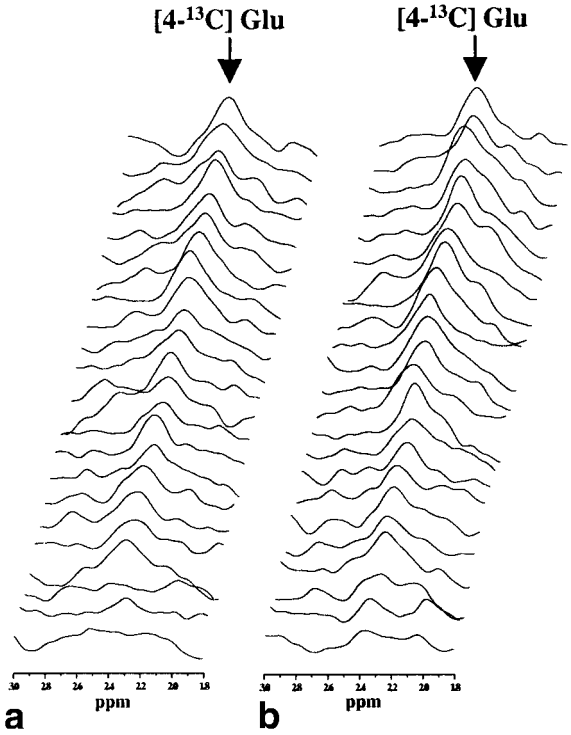

FIG. 3. Stack plots of ^{1}H-{^{13}C} spectra of [4-^{13}C] Glu (3.2-min acquisition time per trace, 6-cm^3 voxel size) after [1-^{13}C] glucose infusion and the hemifield visual stimulation from (**a**) activated and (**b**) control V1 voxels.

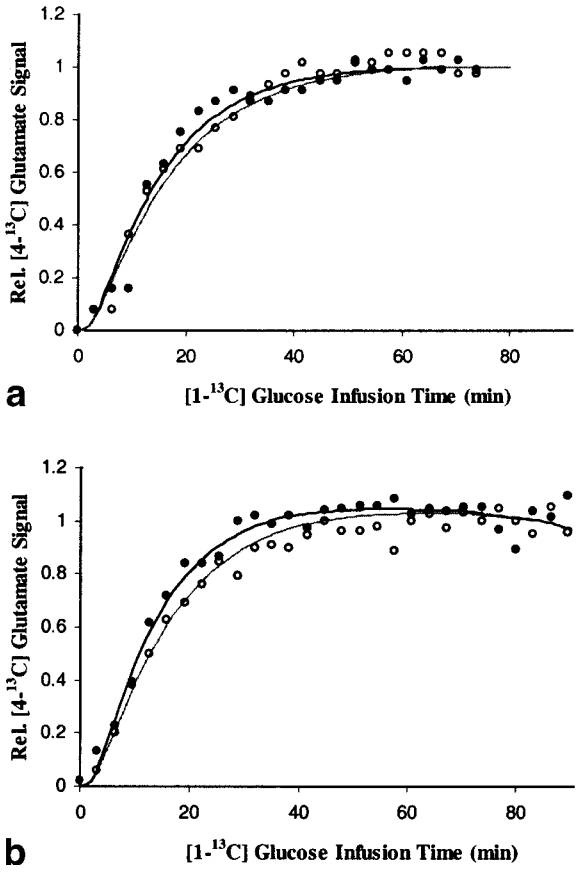

FIG. 4. Turnover curves of [4-^{13}C] Glu isotopic labeling (symbols) and the best fits of the metabolic modeling to the turnover curves (lines). **a:** Results from a single subject (solid circles and solid line: activated V1 voxel; open circles and gray line: control V1 voxel). **b:** Intersubject averaged results (solid circles and solid line: activated V1 voxel; open circles and gray line: control V1 voxel; $N = 5$).

the control side was increased by 28±12% (based on individual subject data, which are summarized in Table 1) or 30% (based on intersubject averaged curve) and this was independent of whether V_x was assumed to be fast relative to TCA cycle turnover rate or equal to it. This 28±12% increase changed to 31±14% after applying partial volume corrections (Eq. [3]).

DISCUSSION

By taking advantage of high sensitivity at high magnetic fields, we have successfully used the two-volume ^{1}H-{^{13}C} MRS method and fMRI to measure metabolic changes coupled to neuronal activity in single subjects within the same experimental session, and from small volumes (6 ml) with a small partial volume effect. The advantage of hemifield stimulation resulted in an inherently paired study, thereby eliminating potential differences in turnover curves between control and activated states when measured at different times and/or subjects. Therefore, these measurements represent a robust estimate of alterations in glutamate turnover, reflecting the actual effect due to brain activation.

Glutamate labeling occurs through the TCA cycle. Taking V_x, the rate of exchange between mitochondrial α-ketoglutarate and cytosolic glutamate, to be either significantly fast relative to TCA cycle turnover rate or equal to it, the fractional increase of V_{PDH} was ~30% (depending on partial volume correction), assuming the effect of a finite turnover of brain glucose on isotope kinetics to be negligible (10). Fractional enrichment kinetics of brain glucose or total brain glucose consumption (CMR_{glc}) rate cannot be measured separately from Glu turnover alone. To assess the influence of brain glucose turnover, we considered the effect of a 50% increase in CMR_{glc}, as reported previously (6), on the ^{13}C enrichment of pyruvate using the reversible Michaelis-Menten model of glucose transport (15). This reduced the calculated change in V_{PDH} to −2±7% (averaged from individual fits) or 1% (when fitting to the averaged time course) without partial volume correction. Assuming a 25% increase of CMR_{glc}, (similar to that reported by ^{1}H MRS from somewhat larger volumes during visual stimulation (22)), yielded an increase in V_{PDH} of 10±10% (averaged from individual fits) or 7% (fitting from averaged data) when glucose turnover was considered in the modeling. It should be stressed that the mathematical covariance between CMR_{glc} and V_{PDH} is expected to result in an increase in CMR_{glc} on the order of 15%, when assuming that all of the glucose is completely oxidized.

Independent of whether the metabolic modeling included glucose label turnover, our study shows that the upper limit on changes in V_{PDH} is ~30%. Assuming the neuronal TCA cycle flux rate to be stochiometrically coupled to CMR_{O2} the study also provides an upper limit in cerebral oxygen consumption measurements. Unless the P:O ratio is altered in the brain during visual activation, the stochiometry of coupling between TCA cycle rate and CMR_{O2} is expected to be constant. A change in the P:O ratio is unlikely to occur in the brain under the conditions of our study. Small changes in the P:O ratio do take place in tissues such as the heart when fatty acids are the dominant carbon source, since fatty acids can act as mitochondrial "uncouplers." However, this is not expected in the brain, where glucose is the dominant carbon source for energy metabolism. Hence, the percentage increase in neuronal TCA cycle rate should be approximately equal to the percentage increases in CMR_{O2} induced by elevated neuronal activity; therefore, our data provide an upper limit of ~30% for CMR_{O2} increase due to visual stimulation.

It is well accepted that the total glucose consumption rate is tightly coupled to CBF at both resting and functionally activated conditions, and both increase ~50% in the V1 areas during visual stimulation (6). Therefore, independent of the constraints and assumptions made in modeling, our results indicate that the CMR_{O2} changes accompanying increases in neuronal activity are not stochiometrically coupled to CBF and CMR_{glc} enhancements. This conclusion is qualitatively consistent with several PET studies (e.g., Ref. 6), and further supports the concept that fractional elevation in glucose consumption exceeds that in the oxygen consumption rate during visual stimulation. The difference may be accounted for by brain glycogen, which is present in significant amounts in the central nervous system (23); however, the quantitative significance of brain glycogen metabolism on these findings remains to be ascertained. If brain glycogen metabolism was unchanged, the results imply that excess pyruvate was formed during visual stimulation, most of which must be exported from the brain cells as lactate. Small increases in cerebral lactate have been reported (17).

In principle, CMR_{O2} can be quantified based on fundamental BOLD theory (e.g., Ref. 24) and/or can be calculated from independent measurements on BOLD, CBF, and cerebral blood volume (CBV) using BOLD modeling (review in Ref. 25). This approach was used for visual stimulation under a single set of conditions, yielding estimates of ΔCMR_{O2} between 5% and 30% (26,27). When graded stimulation was employed (28), similar calculations predicted that fractional increases in CMR_{O2} and CBF are related with a slope of ~0.5. However, experimental determination of all the parameters involved in linking BOLD to CMR_{O2} is so far incomplete, especially in the same subject and under the same set of conditions. The validity of the procedures employed for calibrating some of these parameters using hypercapnia (26–28) remains questionable, since vasodilatation induced by hypercapnia appears to differ significantly from that generated by neuronal stimulation with respect to the type and size of the vessels that are dilated. Despite the ambiguities associated with BOLD modeling, however, the range of results reported by the BOLD modeling are qualitatively in agreement with the relative CMR_{O2} change obtained in the present study.

A previous study reported a large increase of CMR_{O2} of 250% in the somatosensory cortical areas of the anesthetized rat brain during forepaw electric stimulation (10). This CMR_{O2} increase is much greater than the values we observed in the visual cortex of the awake human during visual stimulation, and was much larger than that predicted by most models of the BOLD effect. One possible explanation is that in the resting anesthetized state, the metabolic rates are significantly lower than in the resting awake state, whereas the final values attained during neu-

ronal activation are similar for the anesthetized and nonanesthetized brain (29).

CONCLUSIONS

Based on the quantitative measurements of both metabolic and hemodynamic responses using the ^{1}H-{^{13}C} MRS and fMRI techniques at 4 Tesla in the human visual cortex during hemifield visual stimulation, the fractional change of V_{PDH} and hence CMR_{O2} was less than ~30% and less than fractional increases in CBF. The exact number for V_{PDH}, and hence CMR_{O2} change, however, strongly depend on alterations on glucose-labeling kinetics induced by neuronal stimulation and consequent increase in total glucose consumption rate. Irrespective of this confounding factor, it is possible to conclude that the coupling between CMR_{O2} and CBF changes during focal physiologic neural activity in the human brain is less than unity. This supports the notion that alterations during functional activation would lead to a decrease in regional deoxyhemoglobin content and, ultimately, a positive BOLD effect in fMRI (Ref. 25 and references therein).

ACKNOWLEDGMENTS

We thank Dr. Peter Andersen and Dr. Ivan Tkac for technical assistance. This work was supported by NIH grants RR08079 (National Centers for Research Resources (NCRR)), NS38070 (W.C.), NS35192 (E.R.S.), NS38672 (R.G.), NS39043 (W.C.), and the Whitaker Foundation (R.G.).

REFERENCES

1. Bandettini PA, Wong EC, Hinks RS, Tikofsky RS, Hyde JS. Time course EPI of human brain function during task activation. Magn Reson Med 1992;25:390–397.
2. Kwong KK, Belliveau JW, Chesler DA, Goldberg IE, Weisskoff RM, Poncelet BP, Kennedy DN, Hoppel BE, Cohen MS, Turner R, Cheng HM, Brady TJ, Rosen BR. Dynamic magnetic resonance imaging of human brain activity during primary sensory stimulation. Proc Natl Acad Sci USA 1992;89:5675–5679.
3. Ogawa S, Tank DW, Menon R, Ellermann JM, Kim S-G, Merkle H, Ugurbil K. Intrinsic signal changes accompanying sensory stimulation: functional brain mapping with magnetic resonance imaging. Proc Natl Acad Sci USA 1992;89:5951–5955.
4. Siesjo BK. Brain energy metabolism. New York: Wiley; 1978. p 101–110.
5. Fox PT, Raichle ME. Focal physiological uncoupling of cerebral blood flow and oxidative metabolism during somatosensory stimulation in human subjects. Proc Natl Acad Sci USA 1986;83:1140–1144.
6. Fox PT, Raichle ME, Mintun MA, Dence C. Nonoxidative glucose consumption during focal physiologic neural activity. Science 1988; 241:462–464.
7. Chen W, Adriany G, Zhu XH, Gruetter R, Ugurbil K. Detecting natural abundance carbon signal of NAA metabolite within 12 cm^3 localized volume of human brain using ^{1}H-{^{13}C} NMR spectroscopy. Magn Reson Med 1998;40:180–184.
8. Rothman DL, Novotny EJ, Shulman GI, Howseman AM, Petroff OA, Mason G, Nixon T, Hanstock CC, Prichard JW, Shulman RG. ^{1}H-{^{13}C} NMR measurements of [4-^{13}C] glutamate turnover in human brain. Proc Natl Acad Sci USA 1992;89:9603–9606.
9. Gruetter R, Seaquist ER, Kim S, Ugurbil K. Localized in vivo ^{13}C-NMR of glutamate metabolism in the human brain: initial results at 4 tesla. Dev Neurosci 1998;20:380–388.
10. Hyder F, Chase JR, Behar KL, Mason GF, Siddeek M, Rothman DL, Shulman RG. Increase tricarboxylic acid cycle flux in rat brain during forepaw stimulation detected with ^{1}H-{^{13}C} NMR. Proc Natl Acad Sci USA 1996;93:7612–7617.
11. Xiong J, Gao JH, Lancaster JL, Fox PT. Clustered pixels analysis for functional MRI activation studies of the human brain. Hum Brain Map 1995;3:287–301.
12. Bandettini PA, Jesmanowicz A, Wong EC, Hyde JS. Processing strategies for time-course data sets in functional MRI of human brain. Magn Reson Med 1993;30:161–173.
13. Bottomley PA. Spatial localization in NMR spectroscopy in vivo. Ann NY Acad Sci 1987;508:333–348.
14. Mason GF, Behar KL, Rothman DL, Shulman RG. NMR determination of intracerebral glucose concentration and transport kinetics in rat brain. J Cereb Blood Flow Metab 1992;12:448–455.
15. Gruetter R, Ugurbil K, Seaquist ER. Steady-state cerebral glucose concentrations and transport in the human brain. J Neurochem 1998;70: 397–408.
16. Mason GF, Gruetter R, Rothman DL, Behar KL, Shulman RG, Novotny EJ. Simultaneous determination of the rates of the TCA cycle, glucose utilization, and a-ketoglutarate/glutamate exchange, and glutamate synthesis in human brain by NMR. J Cereb Blood Flow Metab 1995;15: 12–25.
17. Prichard J, Rothman D, Novotny E, Petroff O, Kuwabara T, Avison M, Howseman A, Hanstock C, Shulman RG. Lactate rise detected by ^{1}H NMR in human visual cortex during physiologic stimulation. Proc Natl Acad Sci USA 1992;88:5829–5831.
18. Mason GF, Rothman DL, Behar KL, Shulman RG. NMR determination of the TCA cycle rate and alpha-ketoglutarate/glutamate exchange rate in rat brain. J Cereb Blood Flow Metab 1992;12:434–447.
19. Shen J, Petersen KF, Behar KL, Brown P, Nixon TW, Mason GF, Petroff OA, Shulman GI, Shulman RG, Rothman DL. Determination of the rate of the glutamate/glutamine cycle in the human brain by in vivo ^{13}C NMR. Proc Natl Acad Sci USA 1999;96:8235–8240.
20. Chen W, Zhu XH, Kato T, Ugurbil K. Spatial and temporal differentiation of fMRI BOLD response in primary visual cortex of human brain during sustained visual stimulation. Magn Reson Med 1998;39:520–527.
21. Kim S-G. Quantification of relative cerebral blood flow change by flow-sensitive alternating inversion recovery (FAIR) technique: application to functional mapping. Magn Reson Med 1995;34:293–301.
22. Chen W, Novotny E, Zhu XH, Rothman D, Shulman RG. Localized ^{1}H NMR measurement of glucose consumption in human brain during visual stimulation. Proc Natl Acad Sci USA 1993;90:9896–9900.
23. Choi IY, Tkac I, Ugurbil K, Gruetter R. Noninvasive measurements of [1-^{13}C]glycogen concentrations and metabolism in rat brain in vivo. J Neurochem 1999;73:1300–1308.
24. van Zijl PC, Eleff SM, Ulatowski JA, Oja JM, Ulug AM, Traystman RJ, Kauppinen RA. Quantitative assessment of blood flow, blood volume and blood oxygenation effects in functional magnetic resonance imaging. Nature Med 1998;4:159–167.
25. Ugurbil K, Ogawa S, Kim SG, Hu X, Chen W, Zhu XH. Imaging brain activity using nuclear spins. In: Maraviglia B, editor. Magnetic resonance and brain function: approaches from physics. Amsterdam: IOS Press; 1999. p 261–310.
26. Kim SG, Rostrup E, Larsson HB, Ogawa S, Paulson OB. Determination of relative CMRO2 from CBF and BOLD changes: significant increase of oxygen consumption rate during visual stimulation. Magn Reson Med 1999;41:1152–1161.
27. Davis TL, Kwong KK, Weisskoff RM, Rosen BR. Calibrated functional MRI: mapping the dynamic of oxidative metabolism. Proc Natl Acad Sci USA 1998;95:1834–1839.
28. Hoge RD, Atkinson J, Gill B, Crelier GR, Marrett S, Pike GB. Investigation of BOLD signal dependence on cerebral blood flow and oxygen consumption: the deoxyhemoglobin dilution model. Magn Reson Med 1999;42:849–863.
29. Shulman RG, Rothman DL, Hyder F. Stimulated changes in localized cerebral energy consumption under anesthesia. Proc Natl Acad Sci USA 1999;96:3245–3250.